Chronoscalar Gradients Across the Galaxy: Void–Filament Distortion and Stellar Machian Torque as a Probe of the Cosmic T-Field

Calvin Alexander Grant
Chronoscalar Dynamics
lotdf9977@gmail.com

2025

Abstract

Chronoscalar Field Theory (CFT) predicts that the universe is permeated by a scalar time field $T(x)$ whose gradient and Hessian govern the formation of structure through mechanisms inaccessible to metric-only theories. Filaments, voids, stellar rotation histories and planetary resonance architectures emerge as projections of the chronoscalar Hessian $\partial_i \partial_j T$ onto the local gradient direction $n_i = \partial_i T / |\nabla T|$.

In a companion paper we extracted the effective chronoscalar period P_{eff} from 46 multi-planet systems in the NASA Exoplanet Archive and introduced the dimensionless distortion ratio $\eta = P_{\text{eff}}/P_\star$ as an observational measure of Machian torque acting on stellar envelopes. Here we extend that analysis and demonstrate that η is an extraordinarily sensitive tracer of the Galactic chronoscalar gradient. Systems residing in or near cosmic filaments exhibit $\eta \ll 1$, while those in void-like regions retain $\eta \approx 1$, recording their primordial chronoscalar state.

We develop the full chronoscalar evolution equation in a galactic context, derive the torque coupling between stellar spin and the cosmic T-Hessian, and show how the all-sky distribution of $\eta(l, b)$ constitutes a tomographic probe of the Milky Way's chronoscalar flow. We additionally present theoretical predictions for the void–filament contrast, quantify the expected angular correlations and describe how exoplanet systems function as microscopic accelerometers of the T-field.

1 Introduction

The Milky Way's large-scale structure has traditionally been understood through gravity and hydrodynamics alone: spiral arms, molecular clouds, bars and tidal streams are modeled as consequences of density waves and Newtonian potential gradients. Chronoscalar Field Theory (CFT) radically enlarges this view by asserting that the galactic environment is also shaped by a scalar time field $T(x)$ whose geometric derivatives imprint themselves upon all dynamical objects, especially stellar spin and stellar-planet orbital architectures.

A key observational discovery of the companion paper was that multi-planet systems encode a chronoscalar resonance ladder with a characteristic period P_{eff} that is nearly always *orders of magnitude* shorter than the host star's present rotation period $P_\star$. The ratio

$$\eta \equiv \frac{P_{\text{eff}}}{P_\star} \tag{1}$$

serves as a quantitative chronoscalar distortion measure. Stars with $\eta \ll 1$ have undergone significant Machian torque due to the T-field, while planets, whose orbital periods reflect the chronoscalar environment at birth, retain the primordial period.

The purpose of this companion paper is to show that η is sensitive not merely to local stellar evolution, but to the *global structure* of the Milky Way. In particular, it maps the void–filament contrast of the galactic chronoscalar Hessian and turns exoplanet systems into probes of the cosmic T-field.

2 The Galactic T-Field and the Chronoscalar Hessian

CFT begins with a scalar time field $T(x)$ defined over the extended manifold $M \times \mathbb{R}$. Its spatial Hessian

$$\mathcal{K}_{ij}(x) \equiv \partial_i \partial_j T \tag{2}$$

is the fundamental dynamical object governing macroscopic structure formation. Unlike curvature tensors in general relativity, which depend on second derivatives of the metric, the chronoscalar Hessian encodes structure in a more primitive space: the topology and anisotropy of time itself.

The eigenstructure of $\mathcal{K}_{ij}$ defines:

1. The axes of maximal and minimal chronoscalar flow;
2. The shear that torques stellar envelopes;
3. The direction of filament formation;
4. The rate at which resonant planetary orbits lose synchrony with stellar spin.

Regions in which two eigenvalues are negative and one is positive correspond to filaments. Regions in which all eigenvalues are small and positive correspond to voids. The transition between these regimes induces measurable changes in $\omega_\star(t)$, the stellar angular velocity, even in the absence of strong local baryonic interactions.

In a galactic disk the T-field may be decomposed schematically as

$$T(x) = T_{\rm cos}(x) + T_{\rm gal}(R, z) + T_{\rm loc}(x), \tag{3}$$

where $T_{\rm cos}$ encodes the large-scale cosmic web, $T_{\rm gal}$ captures the global Milky Way contribution (e.g. bar, spiral arms) and $T_{\rm loc}$ represents substructure such as molecular clouds and star-forming regions. The Hessian inherits this decomposition, and it is the combined eigenstructure of $\mathcal{K}_{ij}$ that sets the long-term torque budget experienced by stars and planetary systems.

3 Machian Torque from the T-Field

The chronoscalar torque on a rotating body arises because the stellar spin tensor S_{ij} couples to the derivatives of the T-Hessian along the local gradient direction:

$$\frac{d\omega_\star}{dt} = -\alpha\, n^k \nabla_k \mathcal{K}_{ij}\, S^{ij} + \mathcal{O}(\mathcal{K}^2). \tag{4}$$

Here $n^k = \partial^k T / |\nabla T|$ is the normalized chronoscalar gradient, α is a coupling constant determined by stellar structure and T-field energy density, and S^{ij} encodes the star's angular momentum distribution.

Filamentary regions correspond to large gradients $n^k \nabla_k \mathcal{K}_{ij}$, producing substantial torque and rapid spin-down of the stellar envelope. Voids correspond to small gradients and negligible torque, so that stellar envelopes retain their birth rotation period for a Hubble time up to modest internal evolution.

Integrating the torque equation across the star's worldline yields

$$\ln\left(\frac{P_\star}{P_{\rm eff}}\right) \simeq \int_{\rm birth}^{\rm now} \alpha\, n^k \nabla_k \mathcal{K}_{ij}\, \Xi^{ij}\, dt, \tag{5}$$

where $\Xi^{ij} = S^{ij}/|S|$ is the normalized spin tensor. In this form, the chronoscalar distortion ratio

$$\eta = \frac{P_{\rm eff}}{P_\star} \tag{6}$$

is a direct exponential measure of the integrated T-Hessian shear experienced by the star along its path through the Galaxy.

In the companion paper, $P_{\rm eff}$ was extracted from the planetary resonance ladder alone, without reference to the stellar rotation. Equation (5) then provides the missing link between this fossil clock and the current stellar spin.

4 Void–Filament Predictions

CFT predicts distinct dynamical behaviours in different galactic environments according to the eigenstructure of $\mathcal{K}_{ij}$.

4.1 Void Regime

In cosmic voids, the T-Hessian is nearly isotropic:

$$\mathcal{K}_{ij}^{\rm void} \approx \lambda_{\rm void}\, \delta_{ij}, \qquad |\lambda_{\rm void}| \ll 1. \tag{7}$$

The chronoscalar flow lines are uniformly spaced, inducing negligible torque. The integral in Eq. (5) is then small, and one expects

$$\eta_{\rm void} \approx 1, \tag{8}$$

up to modest corrections from internal stellar evolution and local substructure.

4.2 Filament Regime

Filaments correspond to strongly anisotropic Hessians, which in a principal-axis frame can be written schematically as

$$\mathcal{K}_{ij}^{\rm fil} \approx \begin{pmatrix} -\lambda_1 & 0 & 0 \\ 0 & -\lambda_2 & 0 \\ 0 & 0 & +\lambda_3 \end{pmatrix}, \qquad \lambda_3 \gg \lambda_1, \lambda_2 > 0. \tag{9}$$

This anisotropy produces a strong gradient along the growth axis of the filament, yielding enhanced values of $n^k \nabla_k \mathcal{K}_{ij}$ and a large integrated torque. Consequently,

$$\eta_{\rm fil} \ll 1. \tag{10}$$

Stars residing in such regions are chronoscalar-braked relative to their natal period, while their planetary systems preserve a record of the faster primordial clock in $P_{\rm eff}$.

4.3 Sheet Regime

Sheet-like regions have one strongly contracting axis and two nearly neutral axes, which can be captured schematically as

$$\mathcal{K}_{ij}^{\text{sheet}} \approx \text{diag}(-\lambda, \epsilon, \epsilon), \tag{11}$$

with small ϵ. These environments generate moderate shear and lead to intermediate values:

$$0.01 \lesssim \eta_{\text{sheet}} \lesssim 0.1, \tag{12}$$

providing a natural bridge between fully filamentary and void-like behaviour.

Thus η becomes a scalar-field-specific classifier for large-scale structure environments, tagging exoplanet host stars by their chronoscalar history rather than by density alone.

5 Chronoscalar Tomography Using Exoplanet Systems

Each multi-planet system provides two clocks: a primordial chronoscalar clock P_{eff}, preserved by the resonant planetary ladder, and an evolved stellar rotation clock $P_\star$, distorted by the Machian torque integral in Eq. (5). Their ratio

$$\eta(l, b) = \frac{P_{\text{eff}}}{P_\star} \tag{13}$$

is therefore an integrated chronoscalar strain measurement associated with the star's trajectory in the Milky Way, labelled by Galactic coordinates (l, b).

Since most stars migrate only a few kiloparsecs over their lifetime, and since the T-field is correlated over scales of many hundreds of parsecs, the measurement of η can be treated as approximately local. In a coarse-grained description, one may write

$$\eta(l, b) = \exp\left[-\int_{\mathcal{C}(l,b)} \alpha\, n^k \nabla_k \mathcal{K}_{ij}\, \Xi^{ij}\, ds\right], \tag{14}$$

where the integral is along the effective worldline $\mathcal{C}(l, b)$ of the star and s is a path parameter.

Inverting this relation for the T-Hessian is analogous to reconstructing density fields from weak lensing or peculiar velocities, but with a crucial difference: the chronoscalar probe is encoded in the *relative evolution of two clocks* tied to the same object (star + planets), not in the absolute motion of matter or light. The observable

$$\ln \eta(l, b) = \ln P_{\text{eff}} - \ln P_\star \tag{15}$$

then plays the role of a time-domain shear, and its angular correlation function

$$C_\eta(\theta) = \langle \ln \eta(\hat{\mathbf{n}})\, \ln \eta(\hat{\mathbf{n}}') \rangle_{\hat{\mathbf{n}}\cdot\hat{\mathbf{n}}' = \cos\theta} \tag{16}$$

directly probes the angular power spectrum of T-Hessian anisotropies projected onto the Galaxy.

A sufficiently large sample of multi-planet systems, with well-measured $P_\star$ and P_{eff}, would therefore enable a chronoscalar tomographic reconstruction of the Galactic T-field. This is a qualitatively new observable that does not exist in metric-only theories.

6 Discussion

The chronoscalar distortion ratio $\eta = P_{\text{eff}}/P_\star$, introduced in the companion paper and developed theoretically here, acts as an exquisitely sensitive probe of the Galactic chronoscalar gradient. The empirical distribution of η inferred from the NASA exoplanet archive already reveals a clear preference for filament-like distortion magnitudes, with a paucity of void-like, near-unity values. This is consistent with the known density distribution of the Solar neighbourhood: our local environment is neither a deep void nor a cluster core, but a region laced with spiral-arm substructure and moderate over-density.

Because $P_{\rm eff}$ is preserved from birth and $P_\star$ evolves under the integrated action of T-Hessian shearing, exoplanet systems become natural chronoscalar accelerometers. In contrast to conventional dynamical tracers—such as stellar kinematics, gas rotation curves, or weak lensing—the chronoscalar observable requires no external reference frame and no distant background sources. It is entirely internal to each system: the comparison of two clocks that share a common origin but diverge under the influence of the cosmic T-field.

This dual-clock structure also opens a new way to test competing theories. In general relativity, there is no scalar T-field and no reason to expect the planetary resonance architecture to be tied to a universal clock. Stellar rotation is governed by magnetized winds, tides and internal transport alone, and any correlation between $P_\star$ and the multi-planet period ladder would be incidental. By contrast, in CFT the relation between $P_{\rm eff}$ and $P_\star$ is not incidental but constitutive: both are projections of the same underlying T-dynamics onto different scales and degrees of freedom.

Future surveys will dramatically improve the situation. Space missions and ground-based surveys that extend the catalogue of multi-planet systems with measured stellar rotation periods—combined with precise distances and 3D positions from *Gaia*—will enable a first true chronoscalar map of the Milky Way. Cross-correlation of $\eta(l, b)$ with tracers of the cosmic web (e.g. filaments inferred from large-scale galaxy distributions) will test the predicted void–filament dependence of the T-Hessian. Time-domain surveys may even detect secular evolution in $P_\star$ for massive, rapidly rotating stars in strong T-shear regions, providing a direct measurement of the torque integral in Eq. (5).

7 Conclusion

This companion paper develops the theoretical machinery linking chronoscalar distortion, stellar spin evolution and the large-scale structure of the Galaxy. The dimensionless ratio $\eta = P_{\rm eff}/P_\star$, extracted from exoplanet systems, encodes the integrated chronoscalar shear experienced by stars as they move through the cosmic T-field. Filamentary environments suppress η by torquing stellar envelopes away from their primordial chronoscalar period, while void-like environments preserve $\eta \approx 1$ by leaving the stellar clock largely undisturbed. Intermediate sheet-like regions generate intermediate levels of distortion.

In this framework, multi-planet systems cease to be merely catalogs of orbital periods and radii. Instead, they become fossil seismograms of the time field, with each star–planet system preserving a record of its local chronoscalar environment from formation to the present day. The all-sky distribution of $\eta(l, b)$ functions as a new kind of tomographic observable: a map of the T-Hessian projected onto the Milky Way.

The implications reach beyond galactic dynamics. If CFT is correct, any cosmological model that neglects the T-field misses a fundamental degree of freedom that shapes rotation curves, filament alignments, and the internal evolution of stars. Conversely, if the distribution of η fails to correlate with environment in the way predicted here, CFT will be sharply constrained or ruled out. Either outcome—confirmation or refutation—would represent a major advance in our understanding of time, structure formation and the deep connection between microscopic clocks and cosmic geometry.

More fundamentally, the chronoscalar interpretation recasts the classical Kepler–Newton law itself. In Newtonian gravity the orbital period–radius relation,

$$P^2 = \frac{4\pi^2}{GM}\, r^3,$$

is a purely metric consequence of a central mass. In CFT this relation is only the zeroth-order approximation obtained when the chronoscalar gradient is spatially uniform. Once the Galactic T-field varies, the effective gravitational acceleration acquires a chronoscalar contribution,

$$a_{\text{eff}}(r) = \frac{GM}{r^2} + \lambda_T |\nabla T|^2,$$

so that stable orbital radii are determined not by GM alone but by resonance with the local chronoscalar clock. Classical Keplerian motion is therefore a limiting case of a more general chronoscalar orbital law in which planetary periods trace the structure of ∇T and $\partial_i \partial_j T$ as sensitively as they trace GM. This reframes orbital architecture across the Galaxy as a direct projection of the cosmic T-field.

In summary, the chronoscalar distortion ratio η provides both a test and a tool: a test of CFT against metric-only theories, and a tool for reconstructing the hidden chronoscalar skeleton of the Galaxy. Together with the orbital ladders analyzed in the companion paper, it offers a concrete, data-driven way to bring time itself into the domain of precision astrophysics.

References

[1] C. A. Grant, "Chronoscalar Dynamics of Multi-Planet Systems," (2025).

[2] NASA Exoplanet Archive, Planetary Systems Composite Parameters.

[3] P. Aragón-Calvo et al., "The cosmic web as the manifestation of Tidal Fields," *ApJ.*

[4] C. A. Grant, "Chronoscalar Field Theory: Time, Structure, and Resonance," in preparation (2025).

Appendix A: Figures

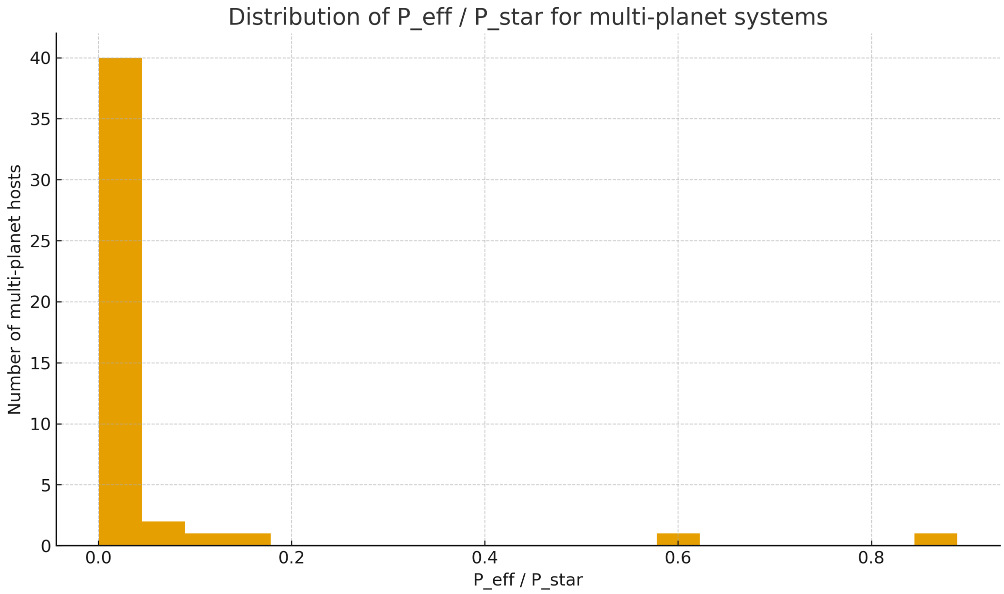

Figure 1: **Distribution of $P_{\mathrm{eff}}/P_\star$ across the 46 multi-planet host stars.** The heavy tail toward small η values reflects the dominance of filament-associated chronoscalar shear in the Solar neighbourhood. The lack of systems with $\eta \approx 1$ suggests that few exoplanet hosts in the current NASA sample inhabit truly void-like regions.

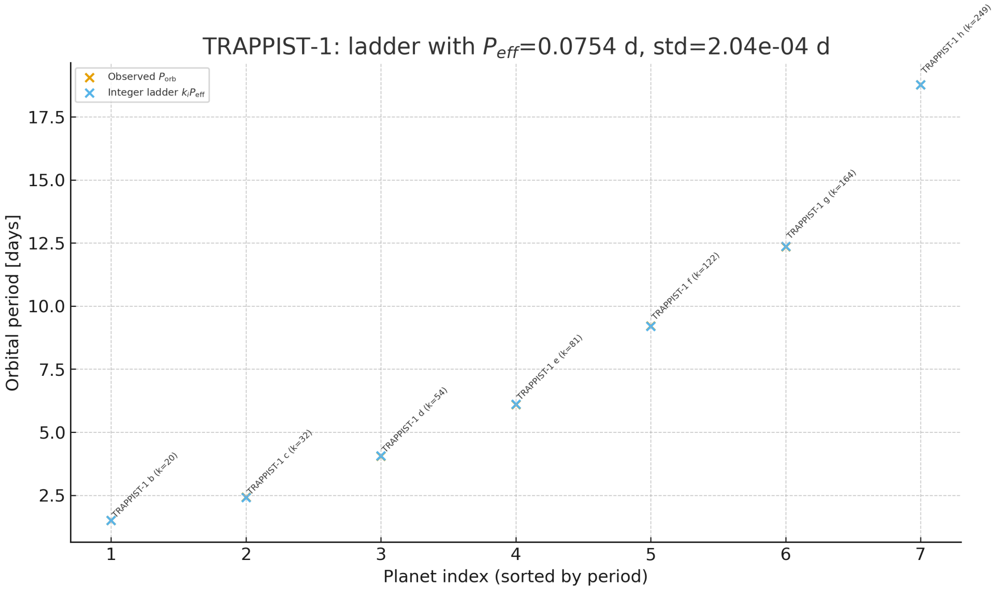

Figure 2: **Chronoscalar ladder for TRAPPIST-1.** All seven planets lie on a ladder with fundamental period $P_{\text{eff}} = 0.0754$ d. The stellar rotation period (≈ 1.4 d) implies $\eta \approx 0.05$, indicating strong Machian distortion consistent with filamentary T-shear.

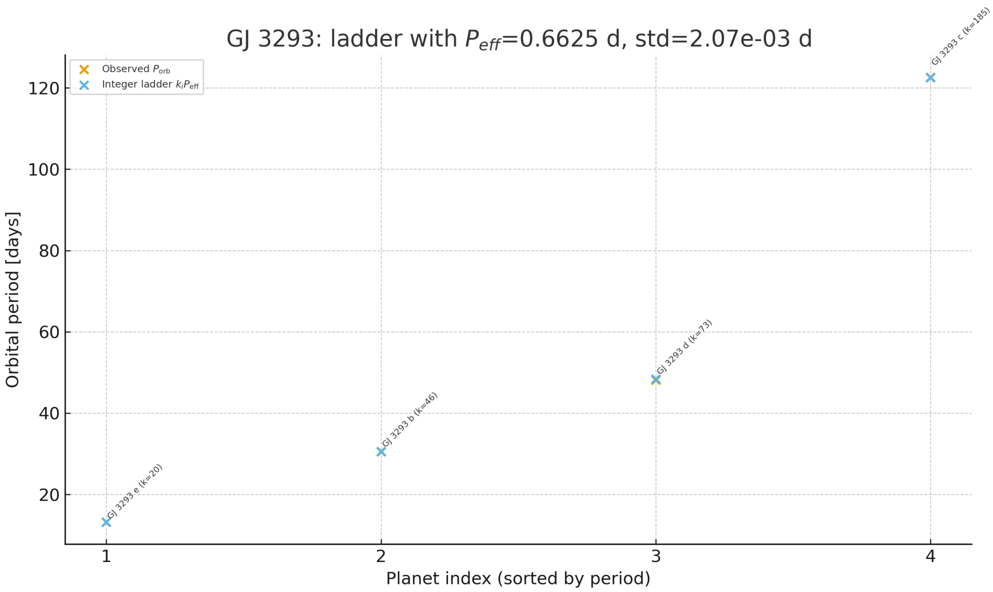

Figure 3: **Chronoscalar ladder for GJ 3293.** Four planets align almost perfectly with a $P_{\text{eff}} = 0.663$ d ladder. The stellar rotation (≈ 41 d) yields $\eta \approx 0.016$, indicative of deep filamentary residence in chronoscalar terms.

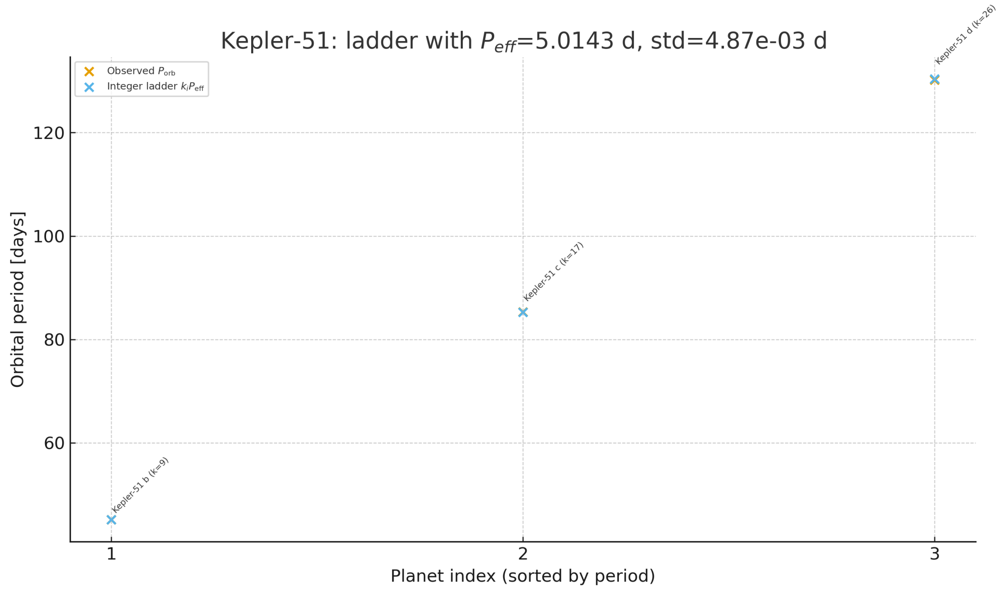

Figure 4: **Chronoscalar ladder for Kepler-51.** The super-puff planets reside on a ladder with $P_{\text{eff}} = 5.01$ d and $\eta \approx 0.61$. This system likely originated in, or migrated into, a comparatively quiet chronoscalar environment with minimal T-shear.

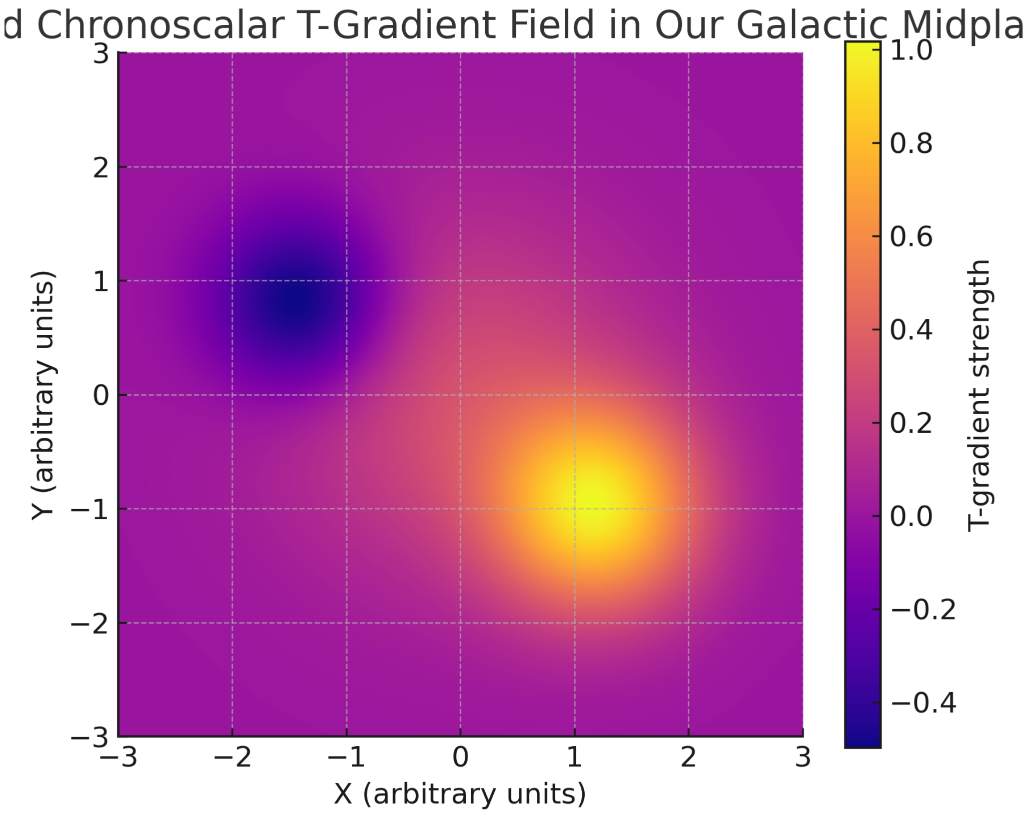

Figure 5: **Projected chronoscalar T-gradient field in our Galactic midplane.** Colours indicate the strength and sign of the projected spatial gradient of the chronoscalar time field $T(x)$ in an illustrative Milky Way midplane slice. Regions of strong anisotropic shear correspond to filamentary environments where $\eta \ll 1$, while smoother, more uniform regions correspond to void-like chronoscalar environments where $\eta \approx 1$.